

NASA TECHNICAL NOTE



NASA TN D-5056

NASA TN D-5056

LITHIUM-DRIFTED SILICON DETECTORS AS LOW-ENERGY PHOTON SPECTROMETERS

by Sherwin M. Beck

Langley Research Center

Langley Station, Hampton, Va.

LITHIUM-DRIFTED SILICON DETECTORS AS LOW-ENERGY
PHOTON SPECTROMETERS

By Sherwin M. Beck

Langley Research Center
Langley Station, Hampton, Va.

NATIONAL AERONAUTICS AND SPACE ADMINISTRATION

For sale by the Clearinghouse for Federal Scientific and Technical Information
Springfield, Virginia 22151 - CFSTI price \$3.00

LITHIUM-DRIFTED SILICON DETECTORS AS LOW-ENERGY PHOTON SPECTROMETERS

By Sherwin M. Beck
Langley Research Center

SUMMARY

Lithium-drifted silicon detectors were fabricated from 10 000 ohm-centimeter, p-type silicon and were tested for use as low-energy photon spectrometers. Three X-ray and gamma-ray sources (Am^{241} , Co^{57} , Cd^{109}) were used to determine the energy resolution. At 77° K and less than 10^{-5} torr (1.33 mN/m^2) the detector resolution varied from 0.82 keV (full width half maximum (FWHM)) at a photon energy of 22.10 keV to 1.04 keV (FWHM) at 122.05 keV with detector-amplifier noise (measured with a pulse generator) almost constant at 0.75 keV (FWHM). From these measurements an intrinsic detector resolution corresponding to a Fano factor of 0.205 was calculated.

INTRODUCTION

The use of solid-state semiconductor detectors in nuclear physics is widespread (refs. 1 to 3). These devices have rapidly progressed from the experimental state to the development level and now enjoy a position of prominence in nearly all recent experiments in low-energy spectroscopy.

In 1960 Pell (ref. 4) demonstrated the possibility of producing a large volume of intrinsic silicon by first diffusing lithium metal into p-type silicon and then drifting the lithium ions through the material. This discovery initiated a surge of activity to develop large diodes with better energy resolution and stopping power than could be obtained from p-n junction detectors in use at that time. Within 2 years the techniques for producing good detectors with depletion regions greater than 5 mm deep were well established for 50 to 100 $\Omega\text{-cm}$, p-type silicon (ref. 5). Diodes with 6.5 keV resolution at full width half maximum (FWHM) for Cs^{137} conversion electrons (625 keV and 655 keV energy) and the same resolution for Pb^{207} X-rays (74 keV and 90 keV) were discussed in reference 5. By 1964, lithium-drifted silicon detectors had been reported with 3 to 4 keV resolution for the same energies (ref. 6). At this time, it appeared that the energy resolution of silicon detectors would be limited by noise in the amplifying systems.

The advent of the field effect transistor (FET) and its applicability to low-noise, charge-sensitive preamplifiers (ref. 7) opened a new phase in the development of

solid-state radiation-detection systems. The degree of success is indicated in more recent publications by Elad and Nakamura (refs. 8 to 10) where 1.5 keV (FWHM) resolution is reported on the 89.4 keV electron line of U^{237} and by Harris and Shuler (ref. 11) where it is reported less than 0.5 keV (FWHM) resolution for 6.4 keV photons of Am^{241} .

The development of lithium-drifted germanium detectors has paralleled that of silicon devices. However, perhaps more effort has gone into producing germanium detectors mainly because of the high mobility of lithium ions at room temperature in germanium which increases the complexity of the fabrication process. Nevertheless Tavendale (ref. 12) reported in 1964 3.1 keV (FWHM) resolution on the 122 keV gamma ray from Co^{57} . Recently Elad and Nakamura (ref. 10) have obtained 0.8 keV (FWHM) resolution on the Co^{57} gamma rays.

The present report is concerned with the performance of lithium-drifted silicon detectors developed at the Langley Research Center for use as low-energy gamma- and X-ray spectrometers. The advantages and limitations of such devices are indicated in comparison with germanium detectors. The results presented herein are based on measurements made in mid-1966 on detectors produced in the first quarter of that year.

SYMBOLS

A	atomic weight
E	photon energy, keV
F	Fano factor
I	photon flux at distance x
mc^2	rest mass energy of electron, 0.511 MeV
N	number of atoms/cm ³
W	line width, same as FWHM
x	distance in detector
Z	atomic number
ϵ	energy required to produce one electron-hole pair
σ	standard deviation for normal distribution

μ attenuation coefficient, cm^2/g

Subscripts:

photo photoelectric effect

compt Compton scattering

pair electron-positron pair production

γ gamma ray

det solid-state detector

photon X-ray or gamma photon

pulser electronic pulser

Abbreviations:

ch channel

EPD etch pit density

eV electron volt (1.602×10^{-19} joule)

FET field effect transistor

FWHM full width at half maximum of a photon peak

Si(Li) lithium-drifted silicon

PHOTON SPECTROMETRY

Photon Absorption in Solid-State Detectors

The absorption and attenuation of electromagnetic radiation in a detector follow the exponential power law:

$$I = I_0 e^{-\mu x}$$

where I_0 is the incident photon flux, I is the photon flux at a distance x from the irradiated surface, and μ is the total attenuation coefficient which is a function of the atomic number of the detector and the incident photon energy. The total attenuation coefficient is a sum of three coefficients associated with photon interactions in matter;

$$\mu = \mu_{\text{photo}} + \mu_{\text{compt}} + \mu_{\text{pair}}$$

where the symbols denote absorption by the photoelectric effect, Compton scattering, and pair production, respectively. The attenuation coefficients for these three interactions have the following dependence on atomic number of the detector and photon energy (ref. 13):

Photoelectric effect:

$$\mu_{\text{photo}} \sim NZ^5/E^{3.5}$$

Compton scattering:

$$\mu_{\text{compt}} \sim \frac{NZ}{E_{\gamma}} \left[\ln(2E_{\gamma}/mc^2) + 1/2 \right] \quad \text{for } E_{\gamma} > 1 \text{ MeV}$$

Pair production:

$$\mu_{\text{pair}} \sim \begin{cases} NZ^2(E_{\gamma} - 2mc^2) & \text{near threshold} \\ NZ^2 \ln E_{\gamma} & \text{at higher energies} \end{cases}$$

The attenuation coefficients (ref. 14) for silicon at photon energies from 10^{-2} MeV to 10 MeV are plotted in figure 1. The total attenuation coefficient for germanium is presented for comparison. For silicon the attenuation process below 0.05 MeV is dominated by the photoelectric effect; between 0.05 MeV and 10 MeV, Compton scattering predominates.

Comparison of the Properties of Silicon and Germanium

Although the absorption of photons by a detector is dependent on the atomic number of the detector material and the incident photon energy, these are only two considerations in choosing a detector for low-energy spectroscopy. In the following discussion the advantages and disadvantages of silicon and germanium detectors for photon spectroscopy below 150 keV are outlined.

The use of lithium-drifted silicon detectors for photon spectroscopy below 100 keV has several advantages. First, silicon detectors can be made with less than 0.5 g/m² dead layer on the entrance window, which allows detection of photons of less than 6 keV energy. The excellent resolution of silicon detectors below 50 keV is possible for several

reasons; the main one is the availability of good quality silicon which permits fabrication of excellent diodes that exhibit almost no energy degradation due to charge trapping by crystal defects. At 77° K some diodes have estimated leakage currents less than 10^{-11} amperes at 500 volts bias. This extremely low current creates a minimum of electrical noise in the amplifying system and consequently increases the energy resolution.

An important practical advantage of silicon devices is their mechanical and thermal ruggedness. Detectors used for this report have been repeatedly cycled between 77° K and 300° K without degradation in resolution or surface properties. This feature greatly facilitates their use and is very convenient in testing new detector-preamplifier configurations. Also, these detectors can be stored at room ambient conditions for extended periods without changes in detector characteristics. The one main disadvantage of silicon detectors is the low atomic number ($Z = 14$) and density which limits their detection efficiency.

Lithium-drifted germanium detectors have several physical properties which make them the ideal choice for photon spectroscopy. Their main advantages over silicon are higher atomic number ($Z = 32$), lower value of energy for the creation of electron-hole pairs, and greater probability of both electrons and holes. Since the photoelectric attenuation varies as Z^5 , germanium is approximately $\left(\frac{32}{14}\right)^5$ more efficient for photon detection than silicon. The greater mobility of both electron and holes in germanium permits faster charge collection and hence greater count rates than in silicon for the same size devices. The lower value of energy for the creation of electron-hole pairs in germanium causes less statistical fluctuation and hence less energy broadening than in silicon.

Although germanium would appear to be the best choice for a low-energy detector, there are several disadvantages and difficulties associated with these devices. The most pertinent is the availability of good germanium crystals. Most commercially obtainable ingots have large defect concentrations which adversely affect detector performance in that the defects act as trapping sites for charge carriers which tend to degrade the energy resolution and to produce a skewing on the low-energy side of photon peaks.

The fabrication of germanium detectors is complicated and time consuming. Germanium crystals are quite brittle and can crack under relatively slight mechanical or thermal stresses. Furthermore, the 0.67 eV band gap requires the use of low temperatures in order to reduce the current flow and resistive heating in the fabrication process. As a consequence, the lithium ion mobility is kept low, and long drifting times are required. After fabrication, detectors must be stored at dry-ice temperatures or below in order to prevent redistribution of lithium ion concentration as noted previously. Also, for maximum performance, germanium detectors must be used at liquid nitrogen temperature in order to suppress thermal creation of electron-hole pairs.

At the present time, all germanium detectors suffer from a relatively thick surface dead layer that attenuates photons below 20 keV and produces a nonlinearity in energy measurements up to 35 to 40 keV. For measurements above 100 keV these problems are negligible and such detectors can give excellent energy resolution. Figure 2 shows a comparison between the intrinsic resolution of silicon and germanium detectors. Data for this figure were taken from reference 11 for silicon and reference 15 for germanium.

APPARATUS

Electronic System

The electronic system, detector mount, and cryogenic system used to obtain the results reported herein are the same as those described by Harris and Shuler (ref. 11). The first stage of a commercial charge-sensitive preamplifier was modified and physically separated from the later stages by approximately 8 cm to permit cooling of the FET. The detector was direct-coupled to a selected type 2N3823 FET, as shown in figure 3. This modification did not significantly affect the characteristics of the preamplifier with respect to rise and decay times, but the noise contribution from the preamplifier was reduced from 1.58 keV (FWHM) to 0.89 keV (FWHM) for zero external capacitance at room temperature. The best noise figure obtained by cooling the front end was 0.63 keV for zero external capacitance.

Signals from the preamplifier were fed to a pulse-shaping amplifier and then to a pulse-height analyzer which had a 3200-channel analog-to-digital converter and a 1600-channel memory. The energy calibration of this system was 0.043 keV/channel for measurements reported herein. The differential and integral linearity was less than 2 percent and 0.1 percent, respectively, over the top 98 percent of the channels. Single differentiation of $6.4 \mu\text{s}$ and integration of $3.2 \mu\text{s}$ were found to be the optimum time constant settings for the amplifier.

Detector Characteristics

All detectors used in the measurements were fabricated with techniques developed at the Langley Research Center. These devices were produced from $10 \text{ k}\Omega\text{-cm}$, p-type, boron doped, float zone purified material. The minority carrier lifetime was greater than 1 ms and the dislocation density as stated by the manufacturer was less than $30\,000/\text{cm}^2$. The wafers were 3 mm thick and 1.8 cm in diameter and cut parallel to the (1,1,1) direction.

From a group of 20 wafers, all cut from the same ingot, six detectors were produced which were considered for use as spectrometers. These detectors have been used periodically over a period of 1 year without any noticeable deterioration in resolution, with the exception that difficulty was encountered in a deterioration of some rear contacts made by

aluminum vacuum deposition. Maximum detector performance can be restored simply by removing the old contact, cleaning the surface, and depositing a new contact. No problems have been noted with the front side and its gold contact. In fact, several detectors were tested with the gold removed from the front sides. No serious degradation in the resolution was noted in such tests.

In figure 4 a cross section of a typical detector is shown and detector characteristics are given. For a description of the detector holder and preamplifier configuration, see reference 11.

RESULTS AND DISCUSSION

Low-Energy Photon Measurements

Three low-intensity X-ray and gamma-ray sources (Am^{241} , Cd^{109} , and Co^{57}) were used to measure the energy resolution of the spectrometer system. As previously noted the system noise at zero external capacitance, as measured by using a precision pulse generator, was 0.63 keV (FWHM).

Photons from the sources were incident on the detector after passing through a 0.25-mm-thick aluminum window in the vacuum system. This window effectively absorbed all photons below 10 keV and probably caused some energy spread in the measurements. No attempt was made to measure this possible error because it was feared that the radiation sources used would outgas and contaminate the cryogenic system if placed inside the vacuum. The spectra shown in figures 5 to 7 were taken with the detectors cooled to 77° K and the system pressure at less than 10^{-5} torr (1.33 mN/m²).

The system resolution varied from 0.82 keV (FWHM) at 22.10 keV (fig. 6) to 1.04 keV (FWHM) at 122.05 keV (fig. 7) with the system noise constant at 0.75 keV (FWHM). This system resolution is sufficient to resolve photon peaks differing in energy by more than 1 keV.

In the next section the intrinsic resolution of the detectors is calculated and a discussion is presented of the importance of statistical fluctuations that occur in the conversion of photon energy to electron-hole pairs in the detector.

Detector Resolution and the Fano Factor

For each charged particle or photon which loses all its kinetic energy E within a solid-state detector, there is an average number N of electron-hole pairs produced in the device. These charges are swept from the detector volume by the electric field produced by the applied voltage, and then into an amplifying system. If the number of electron-hole pairs varies greatly from the average for each particle or photon of the same energy E detected, then the output from the amplifying system will reflect these

variations, which decrease the total energy resolution of the system. For the best energy resolution the variations about the average number of pairs must be a minimum. In principle this minimum variation is defined by Poisson statistics. For example, consider a 36.6 keV particle or photon incident on a silicon detector. The number of electron-hole pairs created is determined by the average energy expended to produce one pair and the particle energy; that is,

$$N = E/\epsilon$$

where $\epsilon = 3.66 \text{ eV}$ (for silicon). Hence, the average number of pairs produced would be

$$N = 36.6 \text{ keV} / 3.66 \text{ eV} = 10^4 \text{ pairs}$$

If the creation of each electron-hole pair is independent of all others, then Poisson statistics predicts a standard deviation about the average number N of \sqrt{N} or

$$\sigma = \sqrt{N} = 10^2$$

For large N , the difference between a Poisson distribution and a normal or Gaussian distribution is negligible. Thus, this number is converted to FWHM in energy terms by the relation

$$\text{FWHM} = 2.355\sigma\epsilon = 2.355\epsilon\sqrt{E/\epsilon} \text{ keV}$$

where the constant 2.355 is the conversion ratio between FWHM and the standard deviation σ of a normal distribution. Hence,

$$\text{FWHM} = 0.928 \text{ keV}$$

is the best resolution possible for a 36.6 keV particle based on statistics. Experimentally the situation is quite different. For example, the detectors used in this report exhibit resolution better than 0.420 keV at this energy. This improved resolution is only possible if the fluctuations about the mean number of electron-hole pairs at a given energy are much less than that predicted by Poisson statistics which, in turn, implies a high degree of correlation between electron-hole pair creation events.

Fano (ref. 15) was the first to point out that such a correlation should exist for particles which lose all their energy in a gaseous detector such as an ionization chamber or proportional counter. The degree of correlation is indicated by a factor F which is the experimental deviation from the mean number of pairs expected from a Poisson distribution. This Fano factor F is usually given by

$$F = \frac{(\text{FWHM})^2}{(2.355)^2 \epsilon E}$$

where FWHM is the detector resolution. A Fano factor of 1 would imply no correlation, that is, Poisson statistics. A Fano factor of 0 would indicate perfect correlation of events; that is, every particle of a given energy would produce the same number of electron-hole pairs and thus the detector resolution would be perfect. Figure 8 demonstrates how the Fano factor affects the resolution of two hypothetical spectrometer systems used to measure closely spaced low-energy photons. All conditions, based on actual spectrometer systems (ref. 11), are assumed to be identical except that detector A has $F = 1$ and detector B has $F = 0.2$. The data used are summarized as follows:

Photon energy, keV	Relative intensity	Detector resolution, FWHM, keV		System resolution, FWHM, keV	
		Detector A	Detector B	Detector A	Detector B
$E_1 = 21.50$	1	0.660	0.295	0.828	0.335
$E_2 = 22.00$	3	.668	.299	.835	.339
$E_3 = 22.50$	2	.676	.304	.841	.341

$F = 1.0$ for detector A, $F = 0.20$ for detector B;
Electronic noise = 0.500 keV (FWHM) for both systems.

The spectrum from system A (for which $F = 1$) gives an indication of multiple peaks and almost no information on the relative intensities. To extract meaningful information from such a curve it must be decomposed to its component parts by a Gaussian curve fitting routine. Such a procedure generally required a computer because of the large number of computations needed to obtain the best fit. Furthermore, the proximity of a high-intensity peak increases the uncertainty in the computed value of the centroid of a smaller peak.

The three photon peaks are clearly resolved by system B ($F = 0.2$). There is no ambiguity in either the energy or intensities. Such a system could detect the presence of two photon sources of equal intensity which differ in energy by 200 eV or less.

The spectra shown in figures 5 to 7 were taken with a detector having a Fano factor of 0.205 (fig. 8) and a pulse-height analyzer and amplifier system which gave a noise contribution of about 0.75 keV, which was almost three times greater than the detector energy spread. Thus, in the measurements shown here, the amplifying system, not the detector, was the limiting factor.

The Fano factor for the detector used here was calculated from the 26.36 keV and 59.57 keV lines of Am^{241} , 22.10 keV line of Cd^{109} , and the 122.05 keV line of Co^{57} . The detector resolution (FWHM) was 0.331 keV at a photon energy 22.10 keV, 0.326 keV at 26.36 keV, 0.474 keV at 59.57 keV, and 0.720 keV at 122.05 keV. Figure 9 shows detector resolution squared $(\text{FWHM})^2$ plotted as a function of photon energy with F as a

parameter. A Fano factor of 0.205 ± 0.012 was obtained from a least-squares fit to the data points. The uncertainty in F is one standard deviation. The error bars in figure 9 are based on the following assumptions:

- (1) A peak of 20 channels full width at half maximum and an integrated area of approximately 10^4 counts can be measured to ± 0.25 channel.
- (2) The differential nonlinearity of the pulse-height analyzer should introduce an error of no more than ± 2 percent in the observed width; for 20 channels this error is ± 0.4 channel.
- (3) The pulse-height analyzer integral nonlinearity of 0.1 percent full scale could introduce an error in the peak width of not more than 0.025 channel for a 20 channel width.
- (4) These errors are independent, hence the uncertainty in peak width is given by

$$\begin{aligned}
 W &= \left[(0.25 \text{ ch})^2 + (0.4 \text{ ch})^2 + (0.025 \text{ ch})^2 \right]^{1/2} \\
 &= \pm 0.472 \text{ ch} \\
 &= \pm 0.472 \text{ ch} / 20 \text{ ch} = \pm 0.0236 \text{ ch/ch} \\
 &= \pm 0.0010 \text{ keV/ch}
 \end{aligned}$$

- (5) Since the square of the detector resolution is given by

$$W_{\text{det}}^2 = W_{\text{photon}}^2 - W_{\text{pulser}}^2$$

the extremes between values of W_{photon} and W_{pulser} , by using the estimated uncertainty in energy per channel, represent a reasonable maximum error for W_{det}^2 . The symbol W_{det} represents FWHM of detector, W_{photon} represents FWHM of observed photon peak, and W_{pulser} represents FWHM of pulser peak.

A Fano factor of 0.205 compares favorably with a Fano factor of 0.26, calculated from data in reference 11 for a silicon detector, and with a Fano factor of 0.166 reported for germanium detectors in reference 16.

CONCLUDING REMARKS

The data presented demonstrate that lithium-drifted silicon detectors can be fabricated with excellent resolution in the energy range below 50 keV. Intrinsic detector resolutions of 0.331 keV at 22.10 keV, 0.326 keV at 26.36 keV, 0.474 at 59.57 keV, and 0.720 keV at 122.05 keV were measured. These measurements were used to calculate a Fano factor of 0.205 which is the lowest value reported to date for silicon. With this detector resolution, the overall resolution of the measurements is presently limited by the noise levels generated in the associated electronic systems.

Langley Research Center,
National Aeronautics and Space Administration,
Langley Station, Hampton, Va., December 18, 1968,
124-09-11-03-23.

REFERENCES

1. Goulding, F. S.: Semiconductor Detectors for Nuclear Spectrometry, I. Nucl. Instrum. Methods, vol. 43, no. 1, Aug. 1966, pp. 1-54.
2. Mayer, J. W.: Semiconductor Detectors for Nuclear Spectrometry, II. Nucl. Instrum. Methods, vol. 43, no. 1, Aug. 1966, pp. 55-64.
3. Hollander, J. M.: The Impact of Semiconductor Detectors on Gamma-Ray and Electron Spectroscopy, Nucl. Instrum. Methods, vol. 43, no. 1, Aug. 1966, pp. 65-109.
4. Pell, E. M.: Ion Drift in an n-p Junction. J. Appl. Phys., vol. 31, no. 2, Feb. 1960, pp. 291-302.
5. Blankenship, J. L.; and Borkowski, C. J.: Improved Techniques for Making P^+-I-N^+ Diode Detectors. IRE Trans. Nucl. Sci., vol. NS-9, no. 3, June 1962, pp. 181-189.
6. Goulding, Fred S.: A Survey of the Applications and Limitations of Various Types of Detectors in Radiation Energy Measurement. IEEE Trans. Nucl. Sci., vol. NS-11, no. 3, June 1964, pp. 177-190.
7. Blalock, T. V.: A Low-Noise Charge-Sensitive Preamplifier With a Field-Effect Transistor in the Input Stage. IEEE Trans. Nucl. Sci., vol. NS-11, no. 3, June 1964, pp. 365-372.
8. Elad, E.; and Nakamura, M.: High-Resolution X-Ray and Electron Spectrometer. Nucl. Instrum. Methods, vol. 41, no. 1, Apr. 1966, pp. 161-163.
9. Elad, E.; and Nakamura, M.: Low-Energy Spectra Measured With 0.7-keV Resolution. Nucl. Instrum. Methods, vol. 42, no. 2, July 1966, pp. 315-317.
10. Elad, Emanuel; and Nakamura, Michiyuki: High-Resolution Beta- and Gamma-Ray Spectrometer. IEEE Trans. Nucl. Sci., vol. NS-14, no. 1, Feb. 1967, pp. 523-531.
11. Harris, R. J., Jr.; and Shuler, W. B.: 500-Volt Resolution With a Si(Li) Detector Using a Cooled FET Preamplifier. Nucl. Instrum. Methods, vol. 51, no. 2, May 1967, pp. 341-344.
12. Tavendale, A. J.: Semiconductor Lithium-Ion Drift Diodes as High-Resolution Gamma-Ray Pair Spectrometers. IEEE Trans. Nucl. Sci., vol. NS-11, no. 3, June 1964, pp. 191-200.
13. Dearnaley, G.; and Northrop, D. C.: Semiconductor Counters for Nuclear Radiations. John Wiley Inc., 1963, pp. 11-12.
14. Davisson, C. M.: Gamma-Ray Attenuation Coefficients. Alpha-, Beta- and Gamma-Ray Spectroscopy, volume 1, Kai Siegbahn, ed., North-Holland Pub. Co., (Amsterdam) 1965, pp. 827-843.

15. Fano, U.: Ionization Yield of Radiations. II – The Fluctuations of the Number of Ions. Phys. Rev., Second ser., vol. 72, no. 1, July 1, 1947, pp. 26-29.
16. Heath, R. L.; Black, W. W.; and Cline, J. E.: Instrumental Requirements for High-Resolution Gamma-Ray Spectrometry Using Lithium-Drifted Germanium Detectors. IEEE Trans. Nucl. Sci., vol. NS-13, no. 3, June 1966, pp. 445-456.

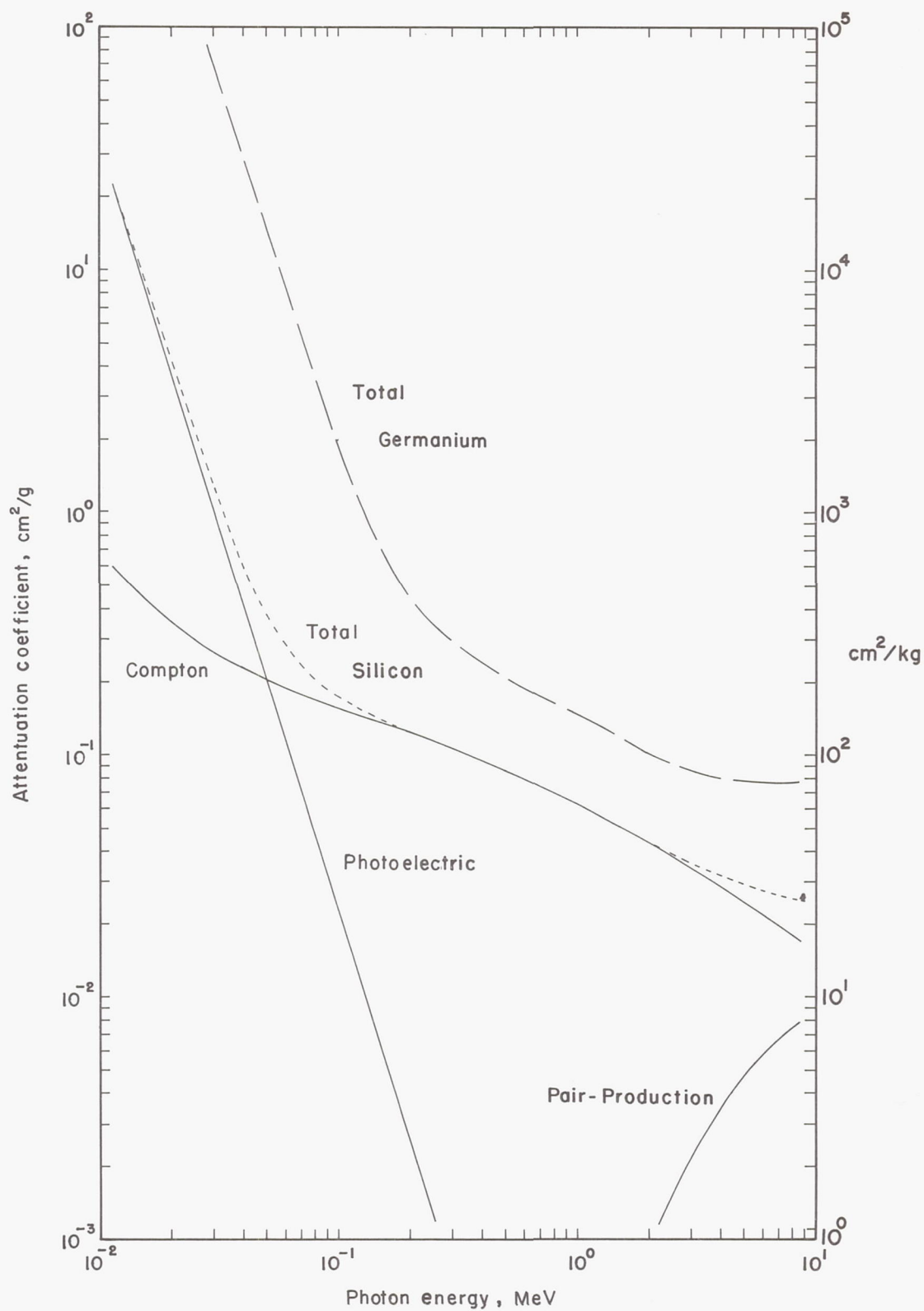


Figure 1.- Attenuation coefficients for silicon and germanium. (From ref. 14.)

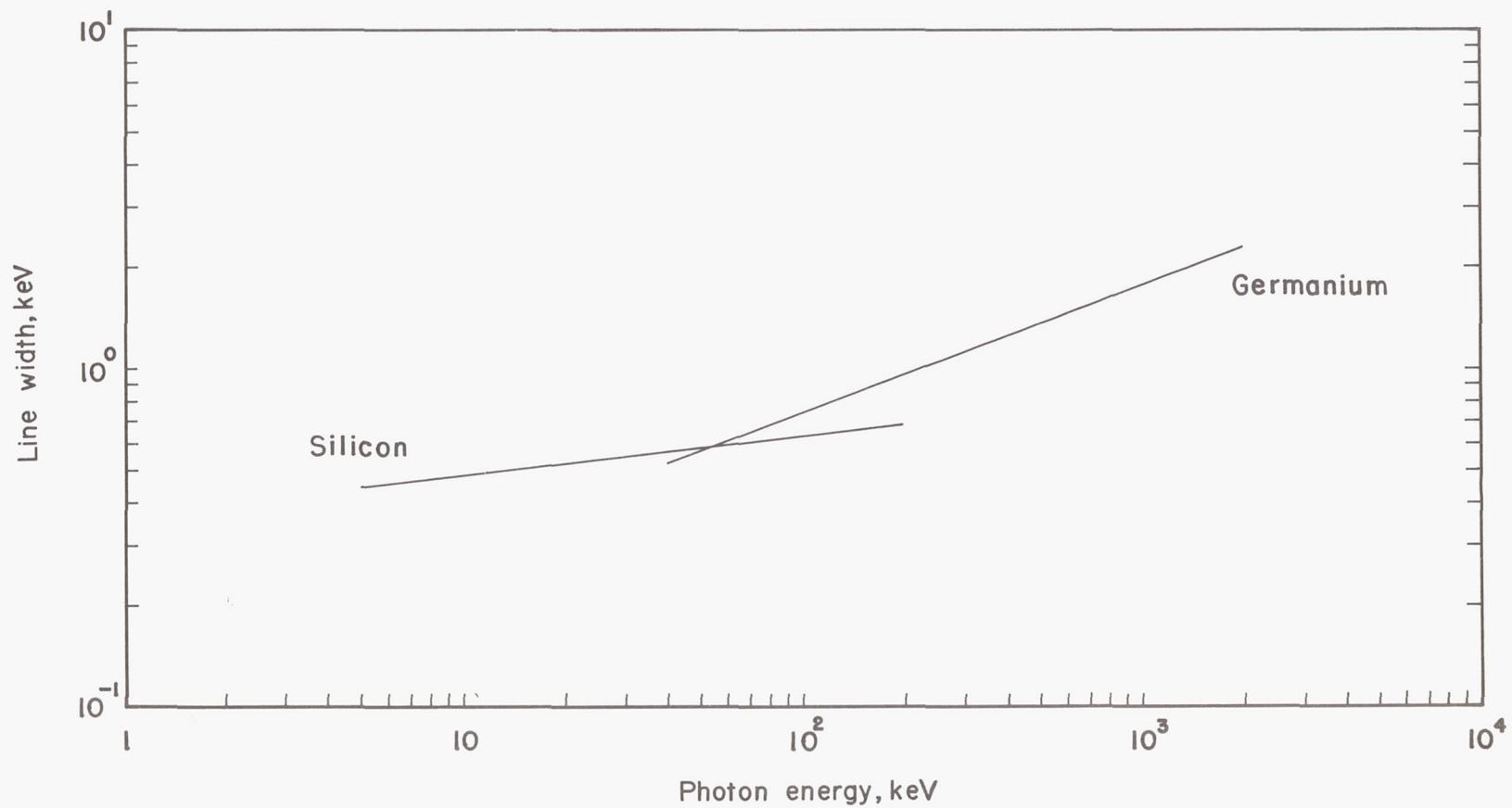


Figure 2.- Comparison between the intrinsic resolution of silicon and germanium detectors. Data for silicon are from reference 11; data for germanium, from reference 15.

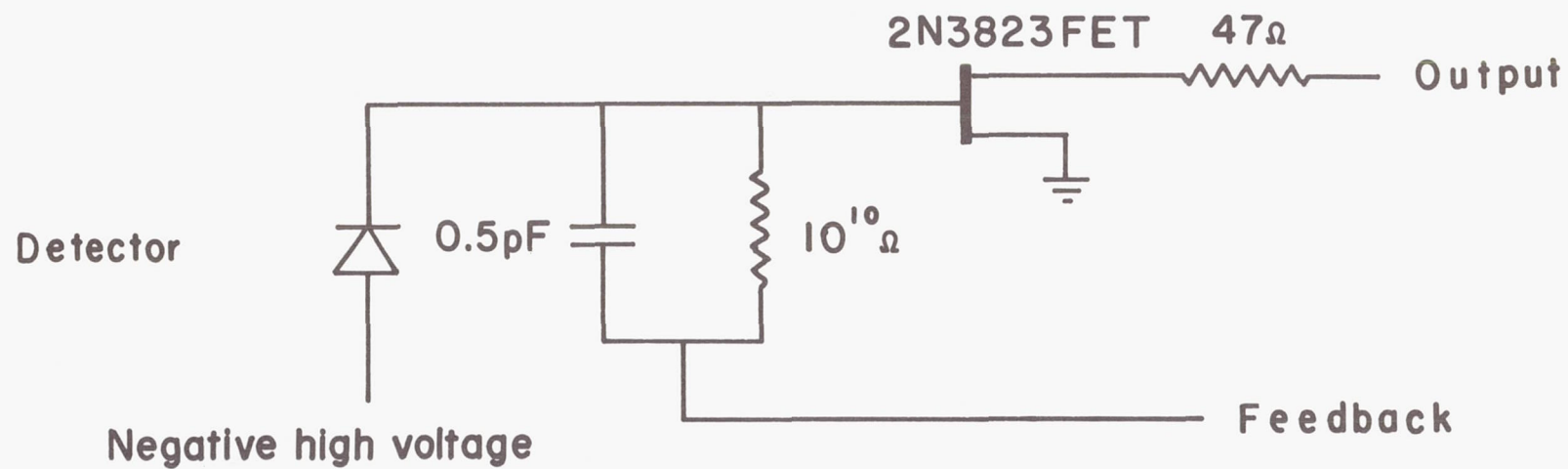
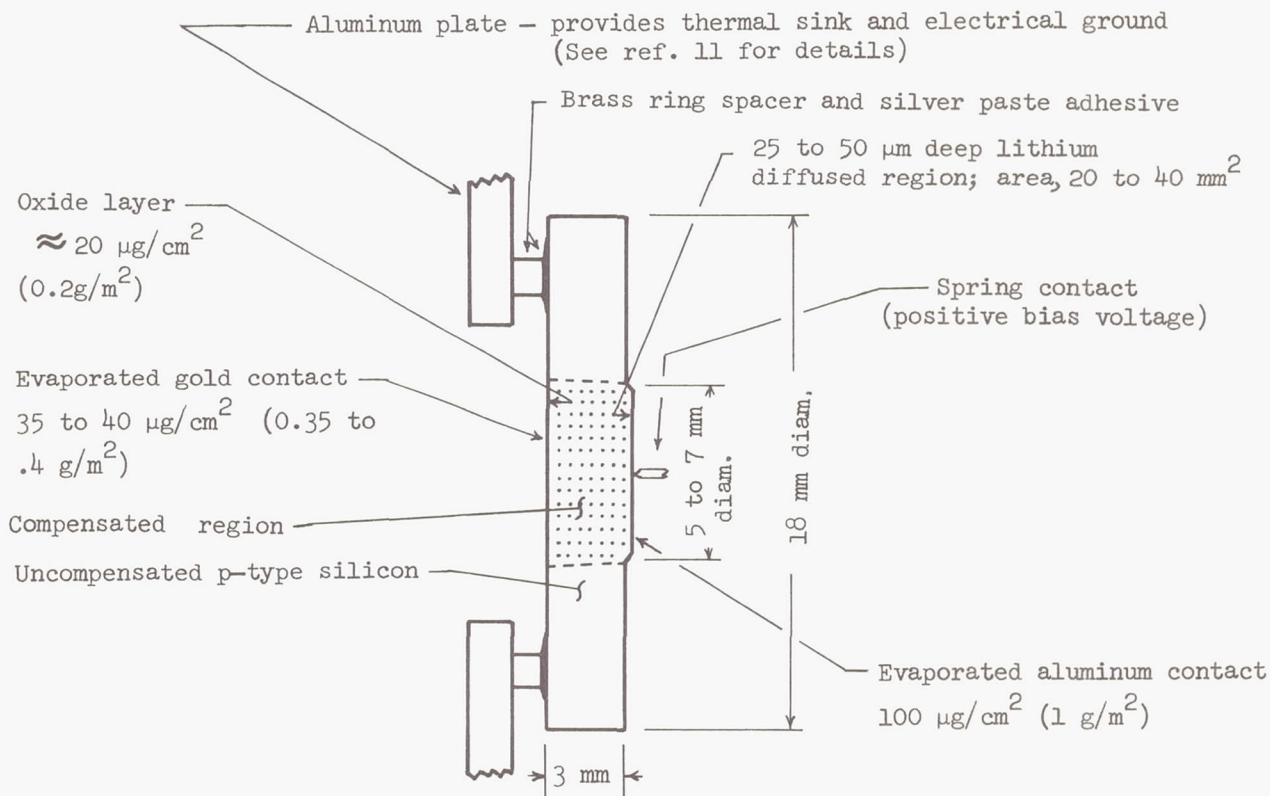


Figure 3.- Detector-preamplifier first-stage configuration.



Detector characteristics:

Silicon: p-type, boron doped, float zoned, (1,1,1) orientation

Resistivity: 10 000 $\Omega\text{-cm}$ ($10 \text{k}\Omega\text{-cm}$)

Minority carrier life-time $\geq 1 \text{ ms}$

Dislocation density: $< 30\,000 \text{ EPD}/\text{cm}^2$

Leakage current at $77^\circ\text{K} \approx 10^{-11} \text{ A}$ at 500 V

Capacitance $\approx 10 \text{ pF}$

Active area: 25 to 50 mm^2

Figure 4.- Detector characteristics.

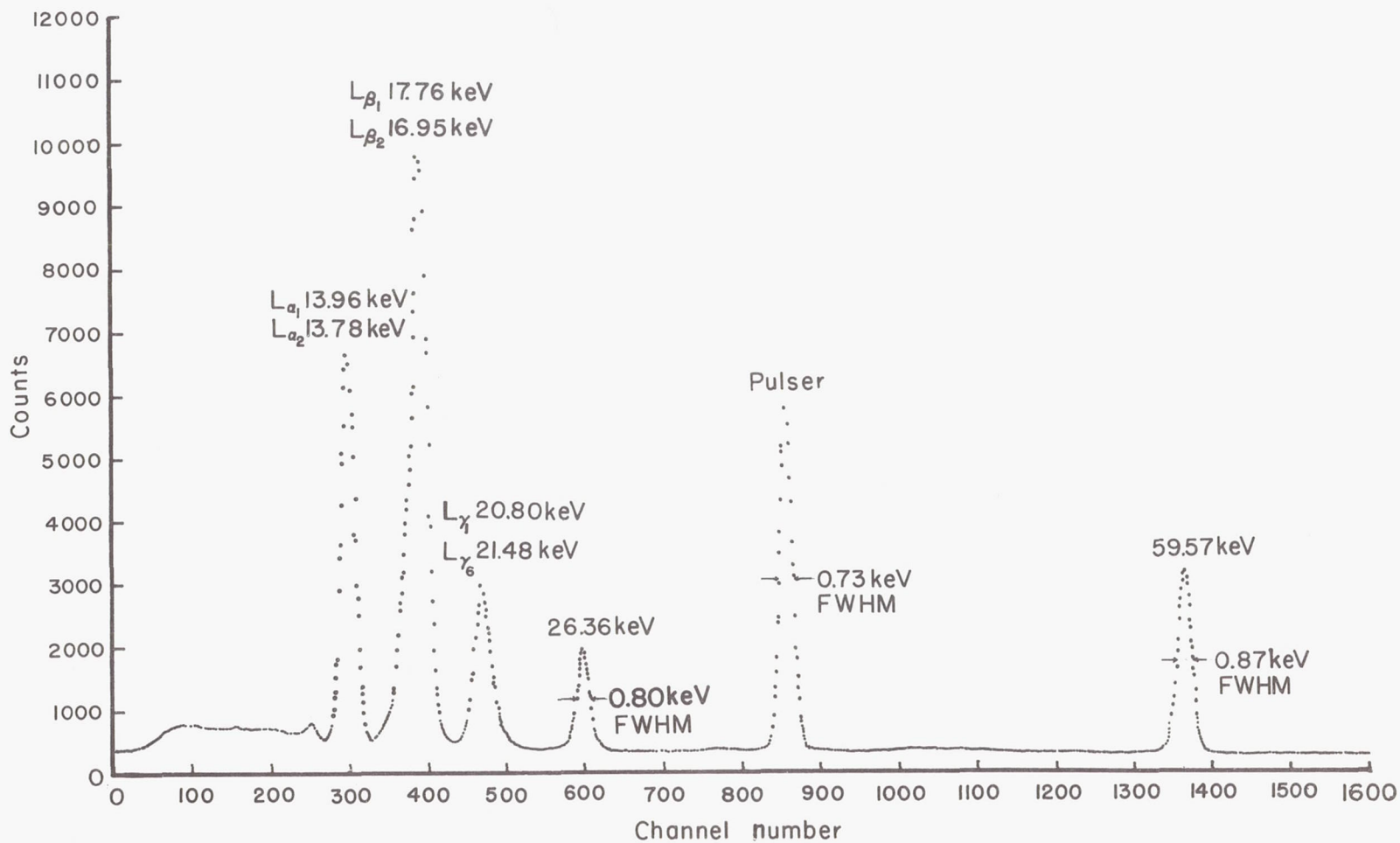


Figure 5.- X-ray spectrum of Am^{241} . Si(Li) detector at 77° K and 490 V bias; energy resolution, 0.043 keV/ch.

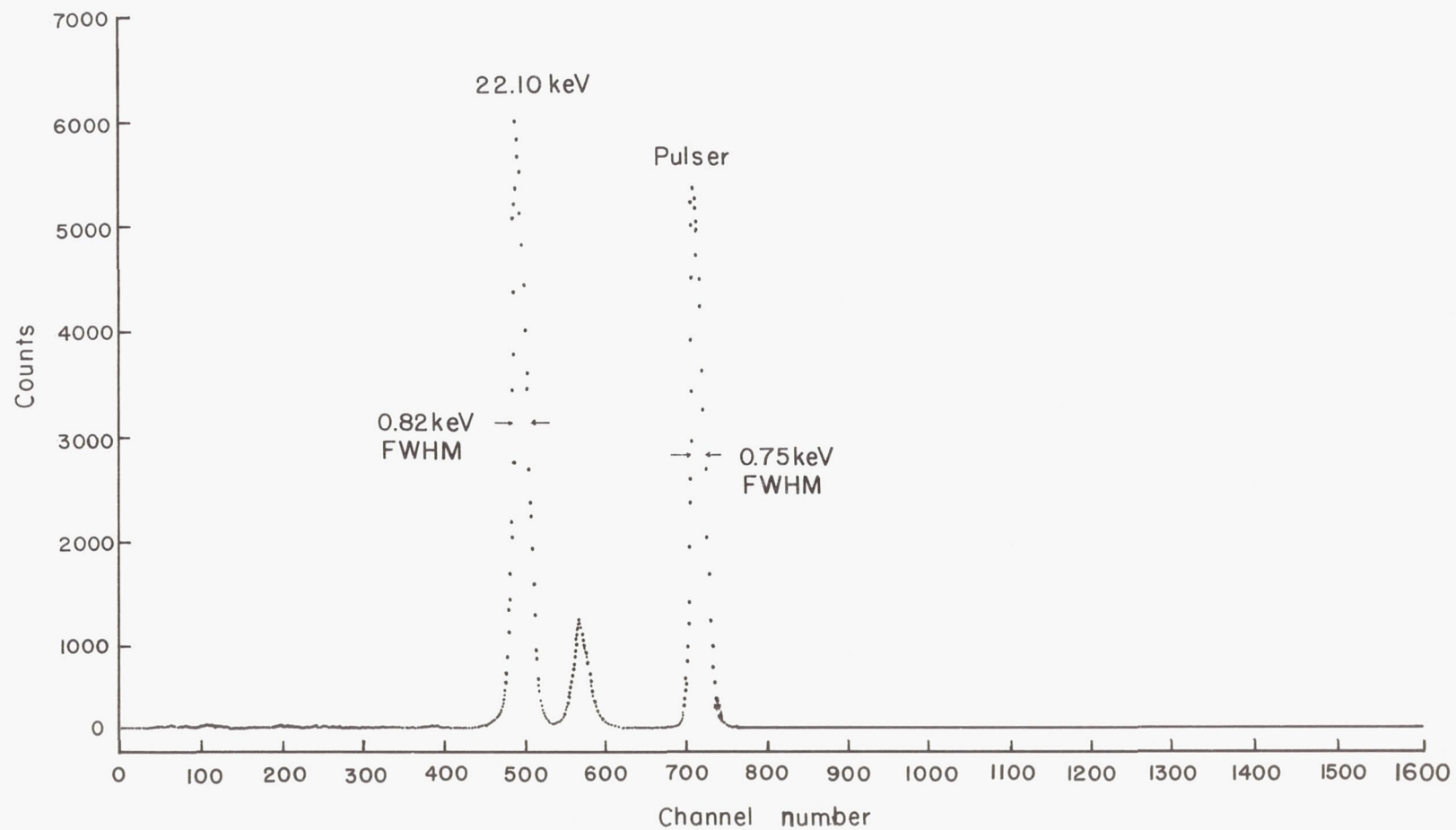


Figure 6.- X-ray spectrum of Cd^{109} . Si(Li) detector at 77° K and 490 V bias; energy resolution, 0.043 keV/ch.

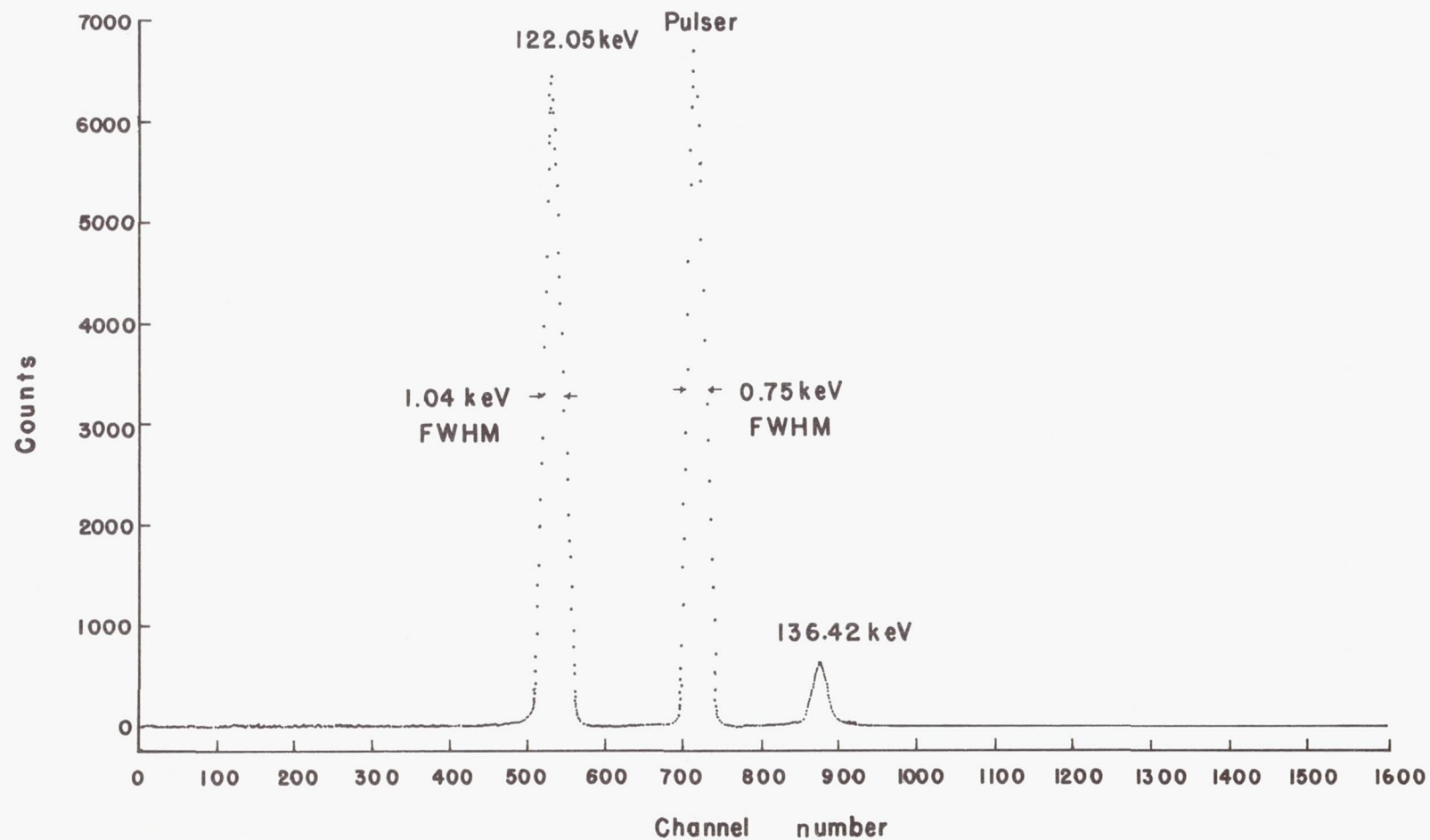


Figure 7.- Gamma rays of Co^{57} . Si(Li) detector at 77° K and 490 V bias; energy resolution, 0.043 keV/ch.

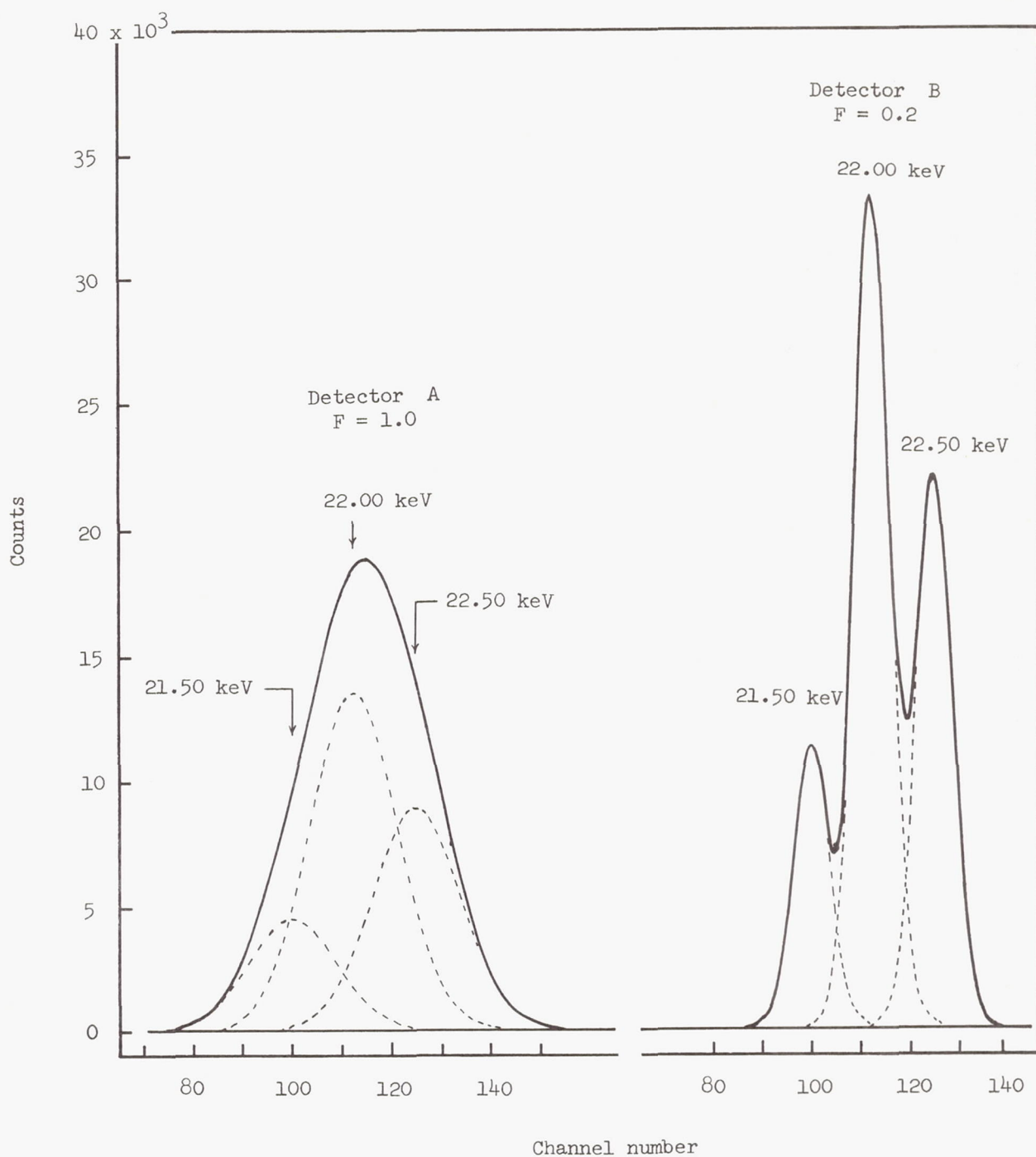


Figure 8.- Effect of Fano factor on resolution.

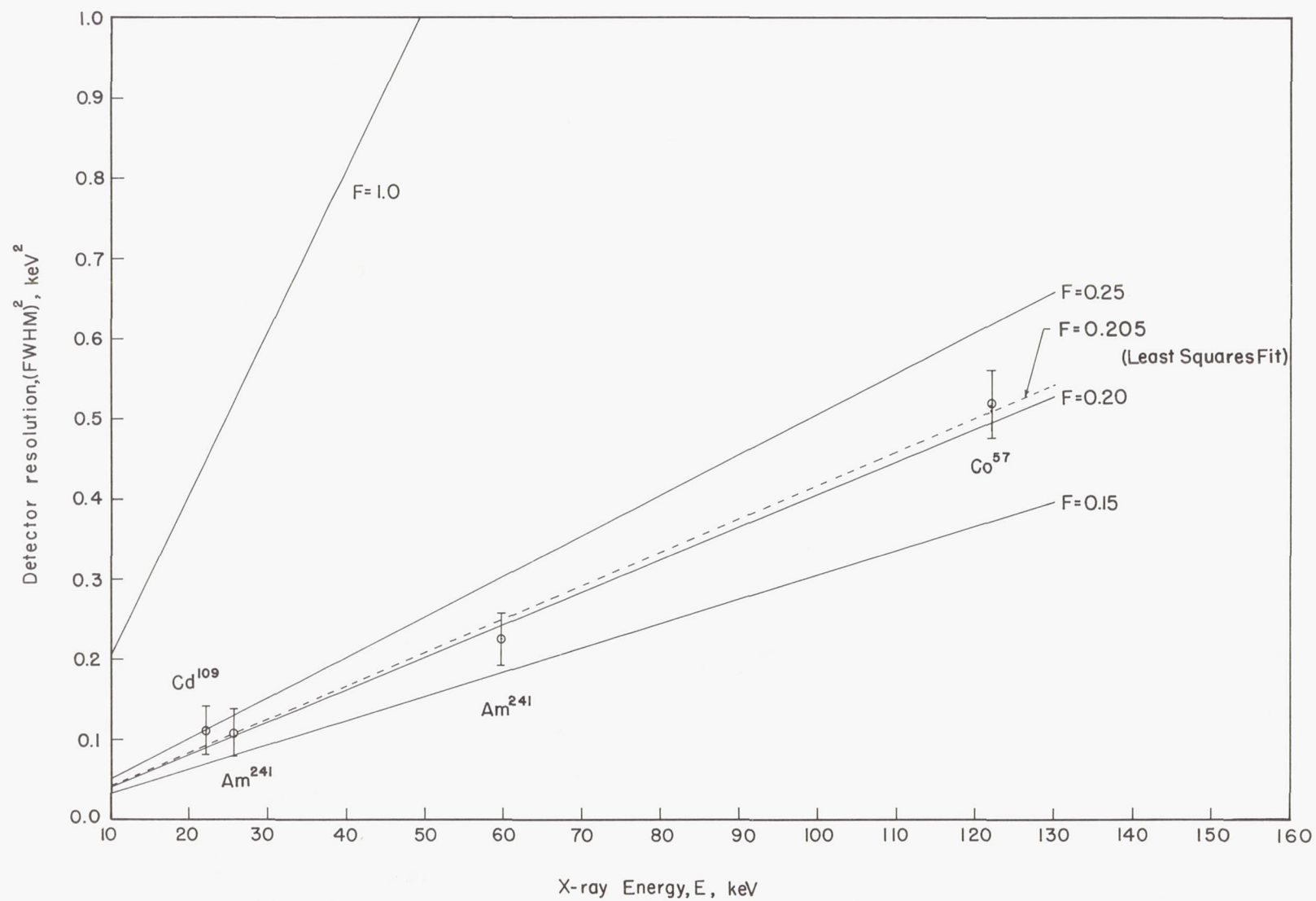


Figure 9.- Fano factor for Si(Li) detectors. $(FWHM)^2 = (2.355)^2 E F$.